Optimization of a synthetic jet actuator for flow control around an airfoil

Optimization of a synthetic jet actuator for flow control around an airfoil

2016 IOP Conf. Ser.: Mater. Sci. Eng. 152 012023

(http://iopscience.iop.org/1757-899X/152/1/012023)

IOP Conf. Series: Materials Science and Engineering **152** (2016) 012023 doi:10.1088/1757-899X/152/1/012023

Optimization of a synthetic jet actuator for flow control around an airfoil

E Montazer[1, 2*], M Mirzaei[1], E Salami[2], T A Ward[3], F I Romli[4] and S N Kazi[2]

[1] Department of Aerospace Engineering, K. N. Toosi University of Technology, Tehran, Iran
[2] Department of Mechanical Engineering, Faculty of Engineering, University of Malaya, Kuala Lumpur, Malaysia
[3] Faculty of Engineering and Physical Science, Heriot-Watt University, Putrajaya, Malaysia
[4] Department of Aerospace Engineering, Universiti Putra Malaysia, Malaysia

[*] elham.montazer@gmail.com

Abstract. This paper deals with the optimization of a synthetic jet actuator parameters in the control flow around the NACA0015 airfoil at two angles of attack: 13° (i.e. the stall angle of NACA0015) and 16° (i.e. the post stall angle of NACA0015) to maximize the aerodynamic performance of the airfoil. Synthetic jet actuator is a zero mass flux-active flow control device that alternately injects and removes fluid through a small slot at the input movement frequency of a diaphragm. The movement of the diaphragm and also the external flow around the airfoil were simulated using numerical approach. The objective of the optimization process function was maximum lift-drag ratio (L/D) and the optimization variables were jet frequency, length of the jet slot and jet location along the chord. The power coefficient of the jet was considered as a constraint. The response surface optimization method was employed to achieve the optimal parameters. The results showed that the actuator is more effective for post stall angles of attack that can lead to an enhancement of 66% in L/D.

1. Introduction

Over the past decade, there has been a growing interest in small active flow control devices that have a significant impact on flow field, and modified forces and momentum around lifting surface, especially for low-Reynolds number applications such as Unmanned Aircraft Vehicles (UAVs). Extensive experimental work has shown that the synthetic jet actuator is an effective way to modify aerodynamic specifications of lifting surface. It can change the structure of vortices near the trailing edge and thus offers potential replacement of conventional control surfaces like flaps [1-5]. Practical implementation of this kind of flow control devices requires experimental development of control systems for aerial vehicles. Recently, the computational tools have been widely used to simulate the flow control. Computational fluid dynamics has provided an insight into the physics of flow control through experimental investigation, which is normally difficult to achieve.

The synthetic jet is also called Zero Net Mass Flux (ZNMF) jet since it is created by oscillating the fluid around the body periodically [3, 6-8]. The net mass flux has been zero since the air surrounding the jet orifice is sucked and blown periodically [9]. The synthetic jet generates momentum difference

that changes the behavior of the flow [6, 7, 10, 11]. Figure 1 shows the most common practical form of the actuator with the output perpendicular to the stream [12, 13]. It is typically consisted of a piezoelectric disk that is attached to a metal diaphragm to form like a sealed cavity [14]. A jet slot is enclosed on one side of the cavity and the diaphragm, which is located in the lower border of the cavity, is deformed by periodic oscillation. During the time that the diaphragm oscillates alternatively, the flow goes into the cavity from the slot and it could be evacuated. In 1998, Smith and Glezer [15] proved that the interaction of the jet with the flow over the surface can displace the local streamlines and induce a virtual change in the shape of the surface.

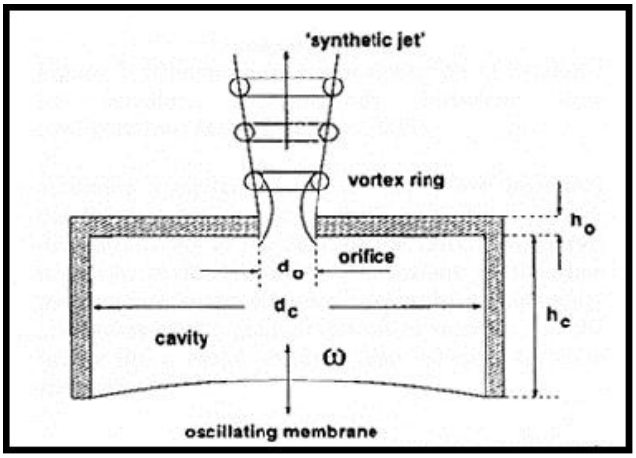

Figure 1. A view of the synthetic jet actuator [12, 13]

In 2005, Holman *et al.* [16] mentioned one of the synthetic jet actuator's ability. It has the ability to integrate the internal flow of the cavity with the external flow without any external device. This makes it an attractive device for flow control in both internal and external flows. Moreover, Ritchie *et al.* [17] demonstrated that the synthetic jet actuators have the advantage of a greater spreading rate than that of the equivalent continuous jet throughout the measured domain at the same time-averaged velocity, thus yielding a greater region of influence on the working domain.

The jet stream can be simulated like a stream with complex spatial and temporal characteristics. Flow typically separates from the edge of the slot and a vortex sheet is formed, which rotated as single and isolated vortices, and subsequently being driven by self-induced velocity. Eventually, the vortices lose their coherence and disappear as they move away from the orifice [18]. The vortices that are created never return to the orifice at suction time, if the synthetic jet can generate the strong velocity.
Recent experimental and numerical studies are testifying that use of synthetic jet actuator as a flow control device is desirable. However, there is still a limited amount of this type of flow control devices that are used on aircraft structures [9]. In recent years, the numerical simulation of the synthetic jets used for stall control around an aerodynamic body has attracted the attention of many researchers. This popularity might be because numerical simulation is a very effective way to explore the possibilities of using synthetic jet on an aircraft [3, 19]. In order to simulate flow control with the synthetic jet, Large Eddy Simulation method (LES) and Direct Numerical Solution method (DNS) for resolving small vortices induced by synthetic jet as they are very convenient [19, 20]. Simulation of the flow with high Reynolds numbers is unfeasible because of high computational cost and difficulties in the simulation. In fact, most numerical simulations for stall control with the presence of the synthetic jet were performed using Reynolds Average Navier Stokes equations method (RANS) [9].

As stated before, one of the main synthetic jet actuator applications is to modify the aerodynamic characteristics of wings and airfoils. Duvigneau and Visonneau [9] demonstrated that the synthetic jet actuator placed on the upper surface of an airfoil is able to modify the streamlines around the airfoil. Lopez *et al.* [2] have reported that using the synthetic jet actuators is an effective way to enhance the lift and modify the momentums of wings and airfoils. Effective control has been achieved using

actuation frequencies with an order of magnitude larger than the natural shedding frequency of the body [2]. An automatic optimization of flow control devices is a sensitive subject due to the drastic computational time related to high accuracy analysis of unsteady flow and the possible multi-constraints of the objective function. The automatic optimization procedure joined with the flow solver is employed by Duvigneau and Visonneau [9] to optimize the actuator's parameters (momentum coefficient, frequency, angle with respect to the wall) at each incidence with the aim of increasing the time-averaged lift. Duvigneau and Chandrashekar [21] used kriging-based algorithms to optimize flow control parameters. These methods are very efficient for global optimization at a reasonable cost. The Response Surface Methodology (RSM) was employed by Tuncer and Kaya [22] for the optimization of periodically flapping airfoil parameters to maximize the thrust generation. The RSM is a collection of statistical and mathematical techniques useful for developing, improving, and optimizing processes in which a response of interest is influenced by several variables and the objective is to optimize this response [23]. It defines the effect of the independent variables, alone or in combination, on the processes [24]. The RSM is discovered to be considerably more proficient than the steepest ascent method. Akcayoz and Tuncer [6] demonstrated that the RSM allows obtaining optimum parameters with similar accuracy by performing a less number of computational evaluations.

This present work deals with the simulation of the synthetic jet actuator located on the section surface of a NACA0015 airfoil as an active flow controller. Unsteady flow over a NACA0015 airfoil is solved using a Navier-Stokes solver. The parametric study demonstrates the synthetic jet parameters must be optimized for improving aerodynamic performance. To the best of authors' knowledge, in literatures, there is no available work dealing with optimization of the jet location, jet frequency and jet slot size. The objective of the optimization is to determine those synthetic jet parameters that maximize the L/D. The RSM is used to find the optimum synthetic jet parameters.

2. Flow simulation and numerical framework

The nature of the flow around an airfoil with the synthetic jet is unsteady and turbulent. Navier-Stokes equations are considered as governing equations. Since Mach number of the free stream is less than 0.3, the flow can be considered as incompressible. The Navier Stokes equations for incompressible two-dimensional flow are:

$$\rho\left(\frac{\partial u}{\partial t}+u\frac{\partial u}{\partial x}+v\frac{\partial u}{\partial y}\right)=-\frac{\partial p}{\partial x}+\mu\left(\frac{\partial^2 u}{\partial x^2}+\frac{\partial^2 u}{\partial y^2}\right)+\rho g_x$$
$$\rho\left(\frac{\partial v}{\partial t}+u\frac{\partial v}{\partial x}+v\frac{\partial v}{\partial y}\right)=-\frac{\partial p}{\partial y}+\mu\left(\frac{\partial^2 v}{\partial x^2}+\frac{\partial^2 v}{\partial y^2}\right)+\rho g_y \quad (1)$$
$$\frac{\partial \rho}{\partial t}+\frac{\partial(\rho u)}{\partial x}+\frac{\partial(\rho v)}{\partial y}=0$$

The turbulent viscosity coefficient is modeled using the Spalart-Allmaras model. The Spalart-Allmaras is a single equation turbulence model that is designed for aerospace applications [25, 26]. For subsonic and incompressible flows, pressure-based SIMPLE algorithm was used to solve the governing equations. An approximation algorithm for velocity was obtained by solving momentum equation. The pressure gradient factor was calculated by pressure distribution in the previous stage or first prediction. The pressure equation was obtained and solved for the new pressure distribution, then the velocity was corrected and new parameter fluxes were found.

2.1. Grid study

Each RANS model requires a suitable mesh that plays an important role in the performance of the model. For this study, C-Type meshing is used. This type of mesh is very convenient for solving flow in flow field that contains vortices. Although there is no specific guideline for determining the size of domain around an airfoil, but a bigger domain as far as the boundaries of the domain do not have an

effect on the solution of the flow field around the airfoil, is the best. When the domain gets bigger, the number of cells in the flow field will also increase and this causes more computational cost. Two-dimensional view of the domain and the size is shown in Figure 2.

Reynolds number based on the airfoil chord length is 896000, the distance between the cells in the direction normal to the airfoil surface starts from 5 to 10 times smaller than the chord length. The first cell size normal to the airfoil surface is approximately two per unit area as shown in Figure 3, which is equivalent to $Y^{+}=2$.

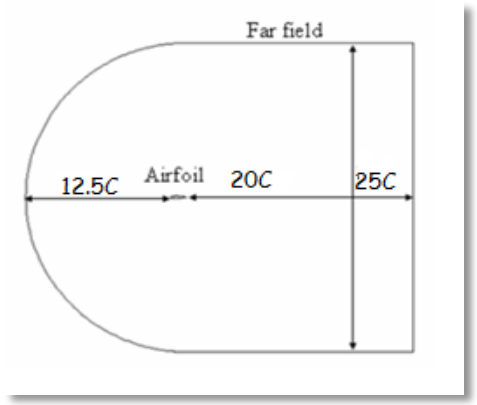

Figure 2. The schematic image of the field around the airfoil

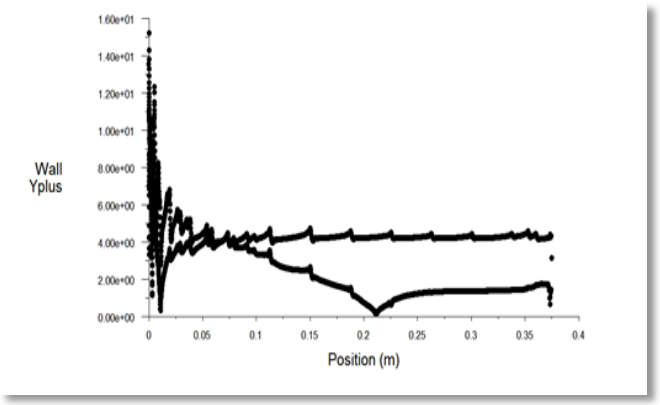

Figure 3. Y+ on the airfoil surface

In order to validate the computational results, they were compared with experimental data reported by Gilarranz *et al.* [12] for NACA 0015 airfoil. Figure 4 shows the comparison for lift coefficient at various angles of attack.

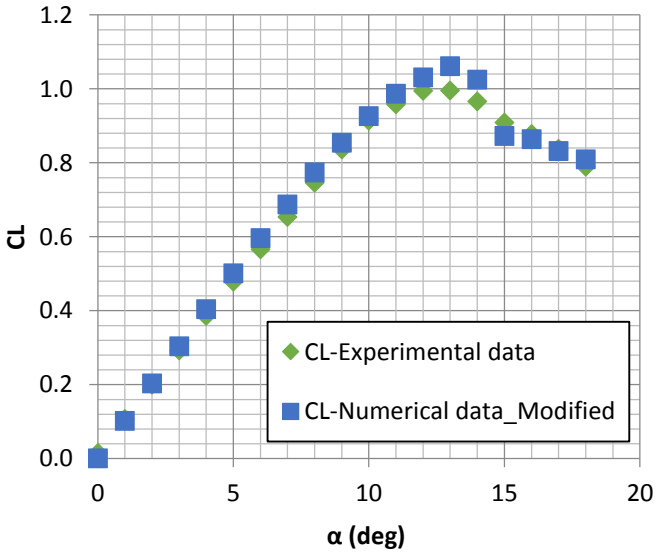

Figure 4. The lift coefficient validation for clean airfoil

As the number of cells that cover the field is increased, the result is more accurate but it should be noted that the increment of the number of small cells causes more computational efforts. Moreover, when the number of cells increases more than the suitable limit, it has no effect on the results. Figure 5 gives a view of domain meshing and clustering of the cells around the airfoil.

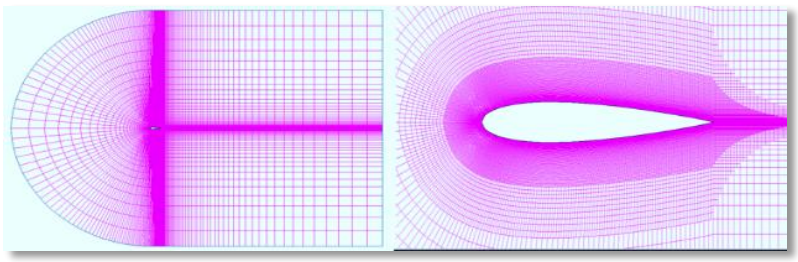

Figure 5. View of the grid in the field and near the airfoil surface

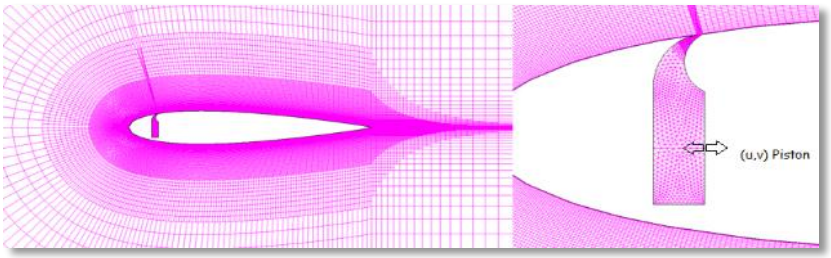

Figure 6. View of the synthetic jet simulation

2.2. Synthetic jet modeling

Previous studies have shown that the size of jet cavity does not play an important role in determining the characteristics of a synthetic jet and it is only an important issue in the modeling of a synthetic jet output flow with higher accuracy [1]. Figure 6 depicts a jet mounted on the upper surface of an airfoil. If the synthetic jet output is tangential to flow, the momentum boundary layer will directly increase. However, if the output of the jet is normal to the wall, it can increase the rate of mixing in shear layer. Gad-El-Hak [19] conducted an extensive review in this area. By utilizing Coanda effect, using a jet with blowing parallel to a wall with large curvatures is possible. He proved that this method is very useful to increase the lift force without requiring moving surfaces.

In the synthetic jet flow dynamics, not only the output flow is important but also the throat that is connecting to the cavity and the outlet is capable of playing a vital role. Based on this observation and the exact dimensions of the synthetic jet slot and the throat, the cavity size can be changed following the actual situation.

2.3. Boundary conditions

In order to simulate the oscillatory motion of the diaphragm, vertical speed set for the diaphragm is obtained as:

$$U_n = A\sin 2\pi F^+ T \tag{2}$$

where F^+ is a dimensionless jet frequency and it depends on the size of the airfoil chord and speed of sound. The experimental jet exit velocity reaches to 85 m/s [13], This velocity is approximately 2.43 times greater than the free-stream velocity ($85 \approx 2.43 U_\infty$). Considering the length of the diaphragm around 22.5 times longer than the jet slot, the maximum amount of diaphragm speed based on the experimental results is estimated $0.108 U_\infty$. F^+ is calculated as:

$$F^+ = \frac{F_{jet} C}{a_\infty} \tag{3}$$

where C is the airfoil chord length and a_∞ is the free stream speed of sound. Lastly, T represents the dimensionless time that is a function of t, U_∞ (free stream velocity) and C: $T = tU_\infty/C$.

Boundary conditions are required for finding an eddy viscosity. The eddy viscosity is dependent on the synthetic jet injected into the main flow, which also plays an important role in the downstream [27]. The turbulent velocity is assumed zero at the cavity's boundaries but still, it is a matter under investigation in numerical simulation of synthetic jet. In order to apply an oscillatory motion of the diaphragm, moving mesh based on mass-spring method was employed to all points on the diaphragm. The maximum of displacement occurred at the midpoint of the diaphragm and the two endpoints were at rest. An appropriate time step for oscillatory diaphragm motion is 0.0001 per second. For each time step, the diaphragm oscillation and cavity mesh should be updated. Figure 7 shows the displacement of the diaphragm and the moving grid points in the cavity.

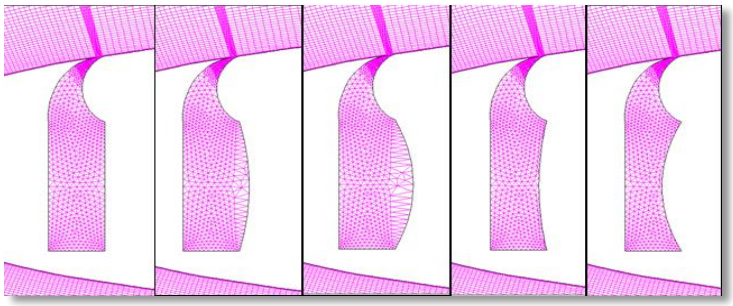

Figure 7. View of the diaphragm and remeshing at different intervals

3. Optimization

In this section, the employed optimization method, namely Response Surface Methodology (RSM), is described. The optimization is based on fitting a response surface model to the data generated by unsteady flow solver for various inputs. The response surfaces are approximated in the defined design space. The optimum design variables that maximize the value of the objective function are estimated using the response surfaces. RSM is a combination of mathematical and statistical techniques, and is based on the generation of response surfaces for a set of design variables [28]. The response can be a function of several variables and it can be obtained using experimental or numerical methods. In the generation of the response surfaces, the method of least squares is employed. Once the response surfaces are determined, the maximum or minimum values of the response and the corresponding values of optimization variables can be evaluated.

In this study, RSM is employed using Minitab software for the optimization of a problem with three optimization variables. A quadratic response surface is the approximated L/D based on the least square method. The quadratic equation for finding the best-fitted curve to numerical data points is:

$$L/D = a_0 + a_1 l + a_2 F + a_3 x_{jet} + a_{11} l^2 + a_{22} F^2 + a_{33} x_{jet}{}^2 + a_{12} lF + a_{13} l x_{jet} + a_{23} F x_{jet} \quad (4)$$

where a is a constant coefficient, l is related to the length of the jet slot, F is the actuation frequency and x_{jet} is the location of the synthetic jet. Once the model is created, it is required to check the goodness of the model [29]. The accuracy of the RSM is validated by calculating RSM residuals, which are the difference between the predicted and calculated responses. A perfect fit line represents the ideal design where difference between the response of the RSM model and computed responses is less than 2%.The optimization process followed throughout this study is explained in Figure 8.

An experimental design for fitting a second-order model must have at least three levels of each factor. There is numerous Design of Experiment (DoE) techniques for fitting a second order model, so it is important to choose the suitable design. The design of experiments concerns the distribution of the points in the design space. One of the best methods to distribute is Full-Factorial (FF) design. The point distribution for Full-Factorial (FF) design is shown in Figure 9. As it is illustrated the design

space is covered completely. The requirement to a high number of computations and being limited low order models are the disadvantages of the full factorial design.

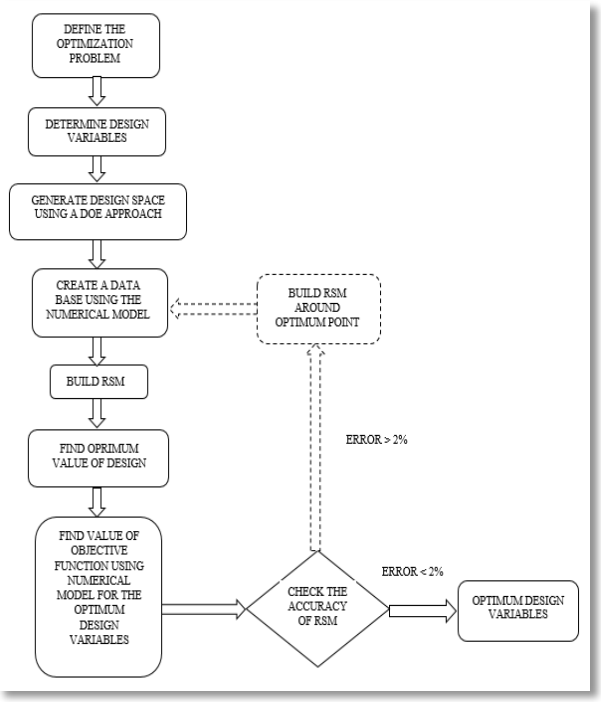

Figure 8. Optimization strategy

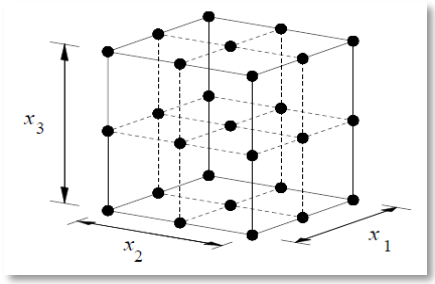

Figure 9. A 33-full factorial sample design

3.1. Optimization of synthetic jet actuator on the NACA0015 airfoil

The optimization was performed at two angles of attack, 13 degrees (that is nearly stall angle of attack of NACA0015) and 16 degrees (post stall angle of NACA0015). The objective function of the optimization was L/D and it was required to maximize this function. As stated before, the jet actuation frequency, length of the jet outlet (slot) and position of the jet slot in the upper surface of airfoil were selected as design parameters. Since the jet inlet and outlet flow are tangential to the airfoil surface, the angle of the jet relates to its location on the surface and the velocity of the jet is dependent on the actuation frequency and the length of the jet outlet. The actuation frequency was varied from 60 Hz to 130 Hz. The jet location on the upper surface of the airfoil was changed ranging from the leading edge to the trailing edge of the airfoil while the jet outlet can have three sizes of 0.6 mm, 1.2 mm and also 4.2 mm.

3.2. Constraints

Power coefficient of the jet was considered as a constraint parameter in the optimization process. Equation 5 shows a correlation between the power coefficient and other flow field parameters.

$$C_{power} = \rho_{jet} L_{jet}^2 u_{jet}^2 F_{jet} \tag{5}$$

where ρ_{jet} is the density of the free stream, L_{jet} is the length of the slot, u_{jet} is the outlet velocity of the synthetic jet and F_{jet} is the actuation frequency. Based on the numerical study conducted by Akcayoz and Tuncer [6], the power coefficient is acceptable when its value is less than 2e-7 during the optimization process.

4. Results and discussions

Optimization is carried out using the RSM. Unsteady turbulent flows over the NACA 0015 airfoil profile were computed using a Navier-Stokes flow solver over a C-grid. The flow was assumed to be fully turbulent and the Spalart-Allmaras turbulence model was employed. In unsteady calculations, the solution was initialized with the free stream conditions. The unsteady computations were carried out until a steady or a periodic behavior in aerodynamic coefficients was observed. The computed flow field was analyzed in terms of pressure coefficient distribution, aerodynamic loads and flow fields over the airfoil.

A parametric study was carried out to investigate the sensitivity of the solution to the synthetic jet parameters. The influence of the jet location, the jet frequency and the length of the jet slot on L/D was investigated. The result of the parametric study was used in the determination of the design space for the optimization study. The synthetic jet parameters were optimized to maximize the L/D. The optimization study was performed at various angles of attack. RSM was employed in the optimization study. The response surfaces for the L/D ratio were approximated using second order model based on the results of the numerical model. The optimum synthetic jet parameters and the corresponding L/D values were estimated using the approximated response surface.

4.1. Optimal control parameters at 13°

The maximum values of the data that correspond to the response surface optimization algorithm in different optimization steps are shown in Table 1. The optimization process was continued until the error gets a value below than 2%. Convergence criterion was satisfied in four optimization steps as shown in Table 1. Figure 10 shows the differences of L/D at 13º with the zero error line. In optimal conditions, the jet velocity reached up to 140 m/s while the inlet flow velocity was 35 m/s, the jet output velocity was approximately four times more than the velocity of the inlet flow. This is a good indicator of the ability of the jet on the airfoil surface and it also leads to improving aerodynamic performance where L/D is more than 28.

Figure 11 shows variation of L/D versus three optimization parameters (length of slot, jet location and actuation frequency), with 3-D surfaces approximated by RSM. Figure 11a shows variation of L/D versus the jet location and the size of the jet slot. The jet location moving between 0.12 m (32% of chord) and 0.15 m (40% of chord) from the airfoil leading edge and the size of the jet orifice varied between 0.001 m and 0.0015 m. In these range of variations, the best and maximum response surface occurred for 13 degrees. Figure 11b displays an area with the jet location moves between 0.075 m (20% of chord) and 0.1 m (26.6% of chord) from the airfoil leading edge and the excitation frequency is varied between 60 Hz to 65 Hz. The figure shows the most optimal area related to these two optimization parameters, but another important parameter that is called the length of jet outlet plays an important role in response and can change this range. Figure 11c indicates the response surface of L/D versus the actuation frequency and the size of the jet slot. The most favorable areas for these two parameters is different from the area obtained by numerical solution at 13 degrees. The difference is explained by the influence of integration of the three parameters with each other and the effect of each parameter on the response surface to define the main area.

Table 1. The optimal result for parameters at 13° in different optimization step

Step	AOA (degree)	Actuation Frequency (Hz)	Length of Slot (mm)	Jet Location (% chord)	Jet Velocity (m/s)	L/D estimated	L/D Numerical simulation	Error (%)
1	13	80	0.6	36	125	26.181	27.190	3.71
2	13	60	0.6	24	130	26.248	27.195	3.48
3	13	60	1.2	36	135	28.097	27.471	2.27
4	13	100	1.2	36	140	27.968	28.244	0.98

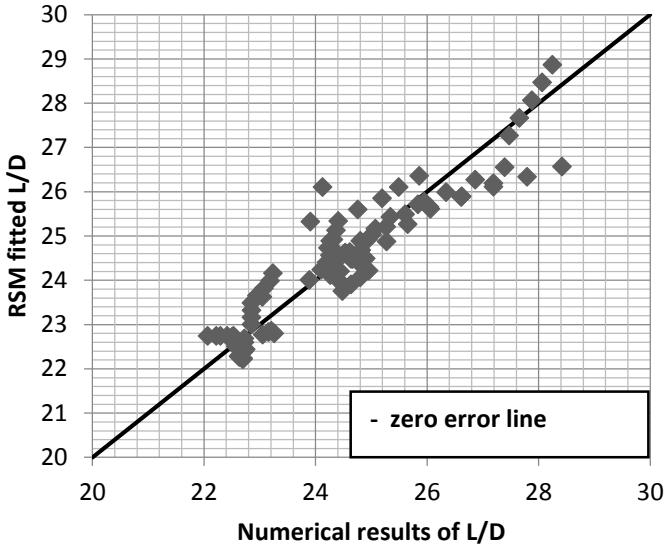

Figure 10. L/D of NACA 0015 estimated from the numerical simulation is in comparison with the fitted L/D obtained by the RSM optimization function at 13°

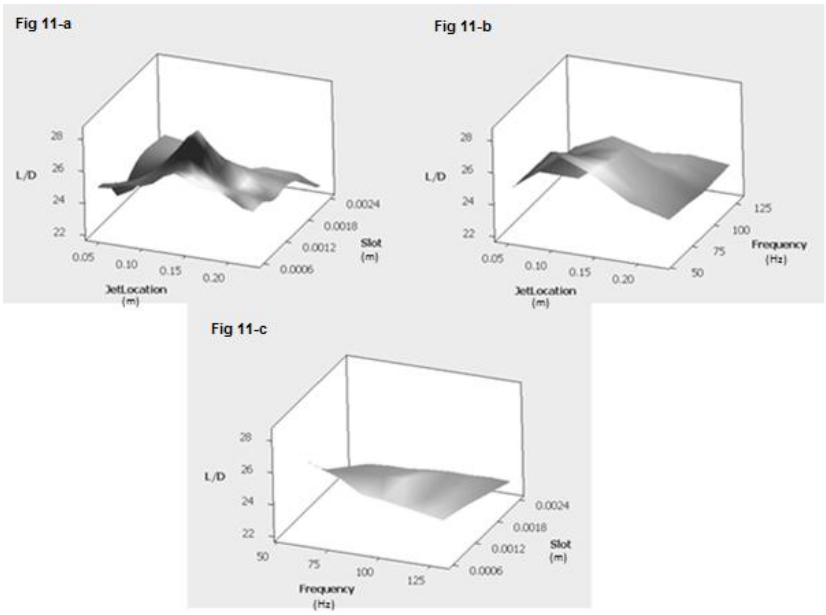

Figure 11. Response surface in 13 degrees for three optimization parameters that vary in exact range

In Table 2, the aerodynamic coefficients of the airfoil at the optimal point are compared with those of a clean airfoil (without actuator). It can be seen that the optimized actuator at stall angle of attack improves the L/D by 29.18% and it can postpone the stall conditions.

Table 2. Aerodynamic coefficients in the angle of attack equal to 13 °

AOA = 13°	**C_L**	**C_D**	**L/D**
Airfoil without synthetic jet	1.061	0.04853	21.864
Airfoil with synthetic jet	1.119	0.03961	28.244
Difference (%)	+5.47	-18.38	+29.18

4.2. Optimization at post stall angle of attack

The optimization study was also performed at $\alpha = 16^{\circ}$, which was a post stall angle of attack for the airfoil. The optimization process was ended in three optimization steps. Table 3 displays the optimum design parameters and relative errors obtained in the optimization steps. The relative difference in the third step was calculated as 1.83%, which satisfied the convergence principles. Figure 12 displays the differences of L/D at 16° with zero error line in third optimization step.

Table 3. The optimal result for parameters at 16° in different optimization step

Step	AOA (degree)	Actuation Frequency (Hz)	Length of Slot (mm)	Jet Location (% chord)	Jet Velocity (m/s)	L/D estimated	L/D Numerical simulation	Error (%)
1	16	60	0.6	12	80	9.973	9.751	2.275
2	16	75	1.2	12	55	7.228	7.684	5.93
3	16	75	0.6	12	85	10.006	9.826	1.83

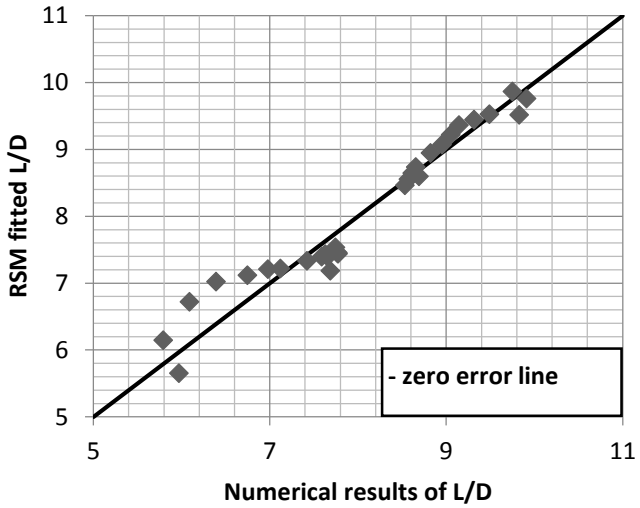

Figure 12. L/D of NACA 0015 estimated from the numerical simulation is in comparison with the fitted L/D obtained by the RSM optimization function at 16°

Figure 13 displays L/D surface approximated by RSM versus the three optimization parameters at angle of attack of 16°. Minimum and maximum points in three-dimensional surfaces were determined. In Figure 13b, an area is clearly marked with containing the jet location varied between 0.3% chord to 24% chord (0.09 m). It shows that the best input frequency range is 60 Hz-90 Hz. The best values of the data that are matching to the response surface optimization algorithm in different optimization steps are indicated in Table 3. The design parameters at optimal condition are: the jet location at 12% chord length, the outlet size is 0.6 mm and the input frequency is 75 Hz. In these conditions, the jet flow velocity reaches to 85 m/s, which is about 2.42 times more than the velocity of inlet flow.

Obviously, the jet has better performance in the post stall situation. A comparison between the aerodynamic coefficients of the optimized actuator with the coefficient of a clean airfoil is given in Table 4. It can be seen that the jet improved the aerodynamic performance of the airfoil more than 66%. This improvement can make the synthetic jet actuator as a suitable controller for active flow control for high angle of attack. According to this comparison, one can find that the effect of the jet on the flow stream in separated flow is more than the attached ones [9]. This can be found in Figure 14. In this figure, the streamlines around the airfoil at the post stall angle of attack were shown. The jet suppresses the recirculating zone and consequently changes the pressure distribution.

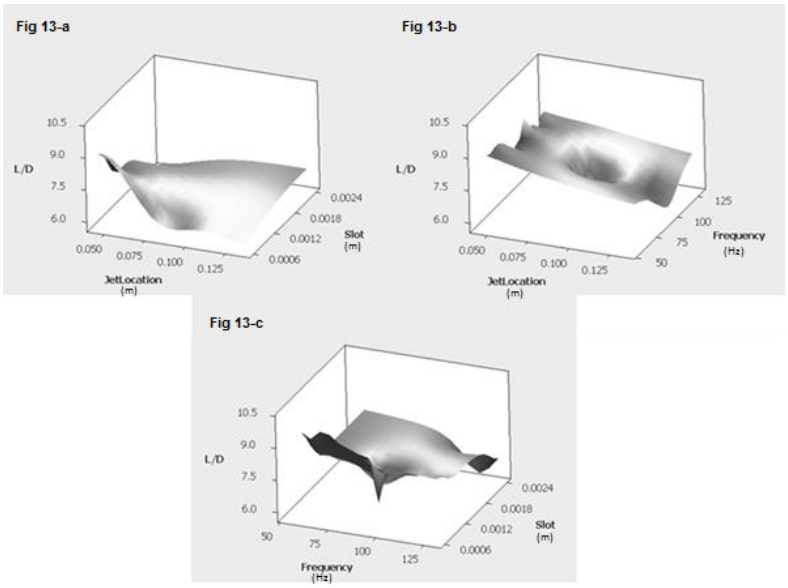

Figure 13. Response surface in 16 degrees for three optimization parameters that vary in exact range

Table 4. Aerodynamic coefficients in the angle of attack equal to 16 °

AOA = 16°	C_L	C_D	L/D
Airfoil without synthetic jet	0.8636	0.1466	5.888
Airfoil with synthetic jet	1.0118	0.1036	9.826
Difference (%)	+17.16	-29.33	+66.88

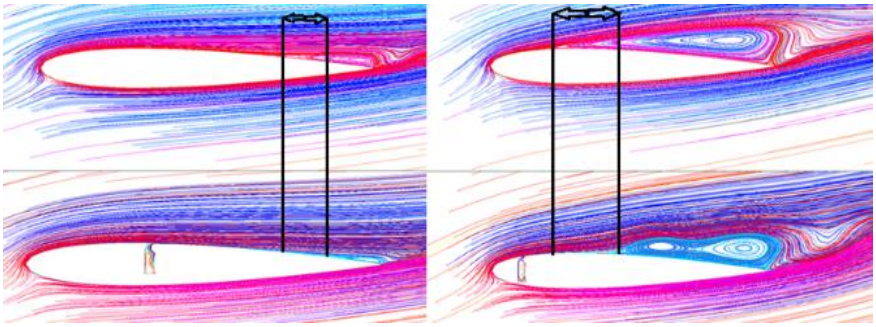

Figure 14. Effect of the synthetic jet actuator for delaying separation in optimal condition, at 13° (left) and 16° (right)

5. Conclusions

The simulation of aerodynamics active control using synthetic jet actuator was performed, solving unsteady Reynolds-Averaged Navier-Stokes equations for NACA 0015 airfoil at Reynolds number, Re = 896000. The flow solver was coupled with the response surface methodology to optimize the jet performance in order to improve the aerodynamic characteristic of the airfoil. The optimization was performed for two angles of attack, i.e. stall and post stall angles of attack. Aerodynamic performance (L/D) was increased by 29% in stall angle of attack and the stall delayed from 13°. Meanwhile, in the post stall angle of attack, L/D had 66% improvement due to reattachment of the recirculation zone on the suction side of the airfoil. The optimum length of the synthetic jet slot was detected to be decreasing as the angle of attack increases. When the angle of attack increased the optimum synthetic jet location was moving to the leading edge. The location of the separation point moved toward the tailing edge on the upper surface as the synthetic jet actuator was used. The optimum actuation jet

frequency and the jet outlet velocity observed to be decreasing as the angle of attack increased from 13° to 16°. Obviously, the synthetic jet was indicated to be the most effective at post-stall angles of attack. It improved L/D significantly and postponed the flow separation.

References

[1] Lopez Mejia O D 2009 *Computational study of a NACA4415 airfoil using synthetic jet control* PhD Thesis University of Texas at Austin
[2] Lopez O, Brzozowski D, Glezer A and Moser R 2009 *19th AIAA Computational Fluid Dynamics Conference*
[3] Patel M, Kolacinski R, Prince T, Ng T and Cain A 2003 *21st AIAA Applied Aerodynamics Conference*
[4] Martin P, Tung C, Chandrasekhara M and Arad E 2003 *21st AIAA Applied Aerodynamics Conference*
[5] Budiyono A, Riyanto B and Park H 2012 *Journal of Aerospace Engineering* **25** 479
[6] Akcayoz E and Tuncer I 2009 *Ankara International Aerospace Conference*
[7] Hamdani H, Baig A and Zahir S 2003 *41st Aerospace Sciences Meeting and Exhibit*
[8] Nassirharand A 2009 *Journal of Aerospace Engineering* **23** 105-10
[9] Duvigneau R and Visonneau M 2006 *Computers & Fluids* **35** 624-38
[10] Yousefi K, Saleh S R and Zahedi P 2013 *International Journal of Engineering* **7** 10-24
[11] Mallison S, Hong G and Reizes J 1998 *13th Australian Fluid Mechanics Conference*
[12] Gilarranz J, Traub L and Rediniotis O 2005 *Journal of Fluids Engineering* **127** 377-87
[13] Gilarranz J, Traub L and Rediniotis O 2005 *Journal of Fluids Engineering* **127** 367-76
[14] Gallas Q, Wang G, Papila M, Sheplak M and Cattafesta L 2003 *41st Aerospace Sciences Meeting and Exhibit*
[15] Smith B L and Glezer A 1998 *Physics of Fluids* **10** 2281-97
[16] Holman R, Utturkar Y, Mittal R, Smith B L and Cattafesta L 2005 *AIAA Journal* **43** 2110-6
[17] Ritchie B, Mujumdar D and Seitzman J 2000 *38th Aerospace Sciences Meeting and Exhibit*
[18] Hayes-McCoy D 2012 *Direct computations of a synthetic jet actuator* PhD Thesis Brunel University London
[19] Gad-el-Hak M 2001 *Journal of Aircraft* **38** 402-18
[20] Gad-el-Hak M 1996 *Applied Mechanics Reviews* **49** 365-79
[21] Duvigneau R and Chandrashekar P 2012 *International Journal for Numerical Methods in Fluids* **69** 1701-14
[22] Tuncer I H and Kaya M 2005 *AIAA Journal* **43** 2329-36
[23] Myers R H, Montgomery D C and Anderson-Cook C M 2009 *Response surface methodology: process and product optimization using designed experiments* (Hoboken: John Wiley & Sons)
[24] Baş D and Boyacı İ H 2007 *Journal of Food Engineering* **78** 836-45
[25] Allmaras S R and Johnson F T 2012 *7th International Conference on Computational Fluid Dynamics*
[26] Spalart P and Allmaras S 1992 *30th Aerospace Sciences Meeting and Exhibit*
[27] You D and Moin P 2007 *Annual Research Briefs* Center for Turbulence Research, Stanford University
[28] Montgomery D C 2008 *Design and analysis of experiments* (Hoboken: John Wiley & Sons)
[29] Mavris D 2006 *Introduction to Design of Experiments and Response Surface Methods* Georgia Institute of Technology